A SUPERVISED CLASSIFICATION APPROACH TOWARDS QUALITY SELF-DIAGNOSIS OF 3D BUILDING MODELS USING DIGITAL AERIAL IMAGERY

Laurence Boudet[1] Nicolas Paparoditis[1] Franck Jung[2] Gilles Martinoty[1] Marc Pierrot-Deseilligny[1]

[1] Institut Géographique National - Laboratoire MATIS. 2-4 avenue Pasteur, 94165 Saint Mandé
[2] Ecole Supérieure des Géomètres et Topographes. 1, boulevard Pythagore - Campus Universitaire, 72000 Le Mans

{laurence.boudet; nicolas.paparoditis; gilles.martinoty; marc.pierrot-deseilligny}@ign.fr
franck.jung@esgt.cnam.fr

KEY WORDS: Quality Self-diagnosis, Consistency, Image-based measures, Performance evaluation, Classification, 3D City Models

ABSTRACT:

In the context of 3D building model production or updating, the models have to be manually checked one by one by a human operator in order to ensure their quality. In this paper, we investigate a new approach to perform a quality self-diagnosis of building models in dense urban areas from high resolution aerial images. Hence, we aim at reliably identifying roof facets that do not comply with quality specifications. The self-diagnosis process will highlight potential incorrect facets for their inspection by a human operator. A set of calibrated aerial images enable us to collect positive or negative evidences of roof facet existence and consistency. A particular attention has been paid to the definition of a set of low-level, complementary, robust and consistent image processing measures. Four quality classes have been defined and are used to classify roof facet quality. A supervised classifier and robust decision rules are then applied to perform an effective self-diagnosis according to the traffic light paradigm. Finally, the work in progress leads to a promising quantitative and qualitative evaluation in the context of dense urban areas.

1. INTRODUCTION

1.1 Motivation

Many applications use 3D building models, such as urban environment planning, telecommunications and natural disaster simulations. Automation of 3D building reconstruction from aerial images has been a very active field of research for the two last decades, leading to a large number of automated or semi-automated systems. Automated production of 3D building models is now conceivable over entire cities, especially when 2D building footprints are available, from cadastral maps for instance. Nevertheless, a verification stage is necessary to control the quality of produced data, including shape description correctness, topological consistency, geometrical accuracy and completeness. This quality control is now a key issue to a greater use and an easier maintenance of 3D building models, since it has been done manually so far.

In this paper, we focus on the quality self-diagnosis of individual roof facets, as a first step of the 3D building model assessment in the context of data production, update or verification. In order to produce useful information on this diagnosis, results should be presented according to the traffic light paradigm (Förstner, 1996). It is based on three qualitative identified classes, namely accepted (high quality verified facets), rejected (poor quality verified facets) and undecided (intermediate quality facets). Then, a verification stage completes the self-diagnosis process, in which a human operator only checks the undecided and rejected facets, in order to confirm, edit or delete them. The self-diagnosis process of 3D roof facet quality is based on aerial images and does not depend on the level of automation involved in the reconstruction stage (none, semi or complete) or on the specific algorithm used to produce the building models.

1.2 Related Work

Since intensive researches have been carried out on 3D building model reconstruction from aerial imagery, quantitative and qualitative evaluations have also been achieved (Henricsson and Baltsavias, 1997, Rottensteiner and Schulze, 2003, Durupt and Taillandier, 2006) using visual inspection and/or a high quality ground truth reference. Avoiding the reference need, (Schuster and Weidner, 2003, Meidow and Schuster, 2005) proposed to use another reconstructed scene to compute either absolute or relative quality measures. Quality criteria are based on completeness, robustness, geometric accuracy, and shape similarity according to the reference, in addition to those proposed in (McKeown et al., 2000). These empirical evaluations showed the capabilities of semi-automated and automated systems for the production of 3D building models.

Another approach of evaluation in computer vision is the algorithm performance characterisation in terms of internal evaluation and error propagation. (Förstner, 1994, Förstner, 1996, Thacker et al., 2005) give useful guidelines on this topic. Nevertheless, the presented self-diagnosis process aims at assessing data quality independently from the reconstruction techniques or algorithms. Thus, self-diagnosis is based on observations of the reality and requires the definition of image-based measures. Some examples can be found in the ”hypothesize and verify” approach of 3D model reconstruction, such as (Suveg and Vosselman, 2002, Jibrini et al., 2004, Taillandier and Deriche, 2004) where the best building model is selected among plausible ones, or such as (Kim and Nevatia, 2004, Ameri, 2000) where the building models are confirmed or discarded during a verification stage. The authors generally take advantage of evidences provided either by a Digital Elevation Model (DEM), correlation scores, 3D feature extraction or shadow detection, according to the initial hypothesis generating method. Finally, the decision is taken by thresholding according to a prior knowledge, by maximizing posterior probabilities or by using a supervised classifier (Kim and Nevatia, 2003).

1.3 Overview

In this paper, quality self-diagnosis of 3D roof facets is performed by using overlapping aerial images. The problem of discriminating facets that comply or not with a set of quality specifications results in a three-class solution, namely an accepted, an undecided and a rejected class. Hence, our problem

is expressed as a classification problem. First, an overview of building modelling errors is introduced in the section 2. Then, a set of image coherence measures is defined (section 3.) in order to prove the roof facet existence and to characterize its consistency. Attention is paid to their robustness and their complementarity. Their combination is performed in a supervised classification stage (section 4.). Finally, the algorithm is applied on two datasets in dense urban areas (section 5.), and evaluated by comparing its results with manual labels of the roof facets.

2. 3D ROOF FACET QUALITY ANALYSIS

In this section, we introduce the input dataset which is constituted of 3D roof facets and aerial images. A succinct overview of building modelling errors is provided.

2.1 Data

3D building models are described by a set of 3D planar polygons (the facets) which represents building roofs without small structure elements, such as chimneys or dormer-windows. Each roof facet is described by geometrical properties (a set of 3D vertices, 3D edges and a normal direction) and topological relations (3D connexity and 2D planimetric connexity between the facets). Their quality evaluation is performed by using multiple 25 cm resolution aerial images. They are acquired by a high quality digital frame camera (SNR=300). Each roof is viewed by 8 to 11 images.

2.2 Building Model Error Causes

In dense urban areas, errors in building modelling may occur because of the complexity of roof shapes, the presence of occlusions and vegetation. Besides, a lack of texture (along the roofs or inside the shadow areas) or a low contrast (along the building ridges) may mislead the reconstruction process. Additional external data which are often used, such as cadastral maps, are also error prone. Moreover, as regards to building reconstruction, some robust approaches do not manage some roof shapes while other more general approaches, based on feature detection, produce less robust and unpredictable results. Finally, buildings may have been destroyed, modified or extended between the database production and new image acquisition.

2.3 Building Model Errors

We may consider three kinds of errors in building modelling:

- the non-existence of the corresponding building,
- the shape description incorrectness which corresponds to under-modelling (Fig. 1) and over-modelling errors. It affects the topological relations and the geometrical characteristics of roof facets,
- the geometrical inaccuracy of a 3D facet, either in slope, altimetric location, and/or planimetric delimitation.

In the following, we focus on the verification of individual roof facet consistency including their existence, their shape description correctness and their geometrical accuracy.

3. CHARACTERIZATION OF THE COHERENCE BETWEEN THE IMAGES

In this section, overlapping images are used in order to collect positive or negative evidences of roof facet consistency. Among several image coherence characterization techniques, we use multi-image correlation and feature detection in order to define robust and complementary measures.

3.1 A Texture Coherence Analysis

Multi-image correlation techniques measure the similarity of textures over image-windows in order to get an estimation of the

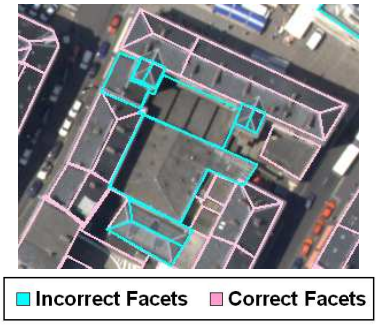

Figure 1: An example of correct and uncorrect (under-modelled) roof facets.

elevation such as in DEMs. Both the correlation scores and the estimated elevations bring an evidence of facet consistency, or on the contrary, find out a better solution.
The multi-image correlation function defined in (Paparoditis et al., 2000) has been selected because it permits to compute efficiently DEMs in a multi-image context with a very low-level analysis (3×3 window size). The image similarity is estimated along the roof facet in the object space. The most probable elevation is estimated by maximizing the correlation function on a scan of a tolerance bound of $[-2m, 2m]$ along the vertical axis. Calling $\mathbf{v_i}$ the vector of intensity values, computed thanks to the implicit homography defined between the images, the multi-image correlation function (MIC) is defined by :

$$MIC = \frac{\text{Var}\left(\sum_{i=1}^{n} \mathbf{v_i}\right)}{\sum_{i=1}^{n} \left(\text{Var}\left(\mathbf{v_i}\right)\right)} \quad \in [0, n] \tag{1}$$

where Var is the variance and n the image number. A preliminary image-window selection stage is performed in order to take into account the occlusions predicted by the building model dataset.

Facet Elevation Consistency Analysis A first clue of roof facet consistency is obtained by measuring the discrepancy between the expected elevation -predicted by the facet- and the estimated one. This difference is shown in Fig. 2.

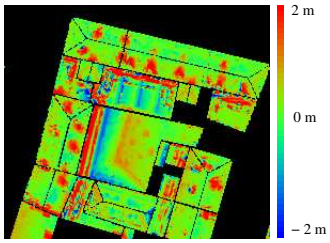

Figure 2: Vertical axis difference between the expected elevation (predicted by the facets) and the estimated one (estimated by maximizing the multi-image correlation function).

Although the under-modelled buildings can easily be identified, it should be noted that occlusions still disturb the elevation estimation. Indeed, occlusion prediction intrinsically depends on the geometric accuracy of the occluding buildings. Besides, elevation estimation is disturbed by the unmodelled roof structures such as chimneys or dormer-windows. Hence, a robust estimator such as the following pseudo-median function is required :

$$\text{med}(Y) = Y\left(\frac{min\left(\mathcal{S}_{\mathcal{F}}, \mathcal{S}_0\right)}{2}\right) \tag{2}$$

where Y is a ranged vector, $\mathcal{S}_{\mathcal{F}}$ is the facet area and $\mathcal{S}_0$ is an area threshold (500 m^2) used to cope with large facets. Hence, a first measure of facet consistency is based on the robust estimation of

the distance between the estimated elevation points $\hat{P}(x, y, \hat{z})$ of each ground pixel (x, y) and their projection onto the facet plane $\mathcal{P}_{\mathcal{F}}$. It leads us to define the Correlation Distance (**CD**) value by :

$$\mathbf{CD} = \underset{(x,y)\in\mathcal{F}}{\text{med}} \left(\mathcal{D}_{\mathbb{R}^3}(\hat{P}(x, y, \hat{z}), \mathcal{P}_{\mathcal{F}}) \right) \quad (3)$$

where $\mathcal{D}_{\mathbb{R}^3}$ is the euclidean distance in $\mathbb{R}^3$.

Correlation Function Profile Analysis Another clue assessing the roof facet consistency is provided by the correlation function profile. Correlation scores along the facets (Fig. 3, on the left) are expected to be high for correct facets and higher than those obtained along the vertical scan of the object space.

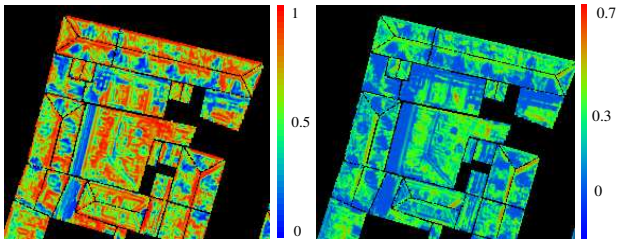

Figure 3: Multi-image correlation function (on the left) and correlation profile function (on the right) applied on the facets.

Two issues linked to the correlation function have to be handled. Firstly, homogeneous or periodic textures result in smoothed correlation profiles or in local extrema. Such profile should not be considered as reliable even if correlation scores are high. Secondly, since an image-window selection stage is carried out to cope with occlusions, the number of images varies from one pixel to another. Thus, a normalisation is required but linearity is not fulfilled. Both of these issues have been getting through by defining a new consistency measure based on the shape of the correlation profile (Fig. 3, on the right). It takes into account the correlation score $s_{\mathcal{F}}(x, y)$ obtained near the facet and its relative differences with the scores $s(x, y, z)$ obtained along the profile, where (x, y) is a ground pixel. Applying the pseudo-mediane function, we define the Correlation Profile (**CP**) value by:

$$\mathbf{CP} = \underset{(x,y)\in\mathcal{F}}{\text{med}} \left({s_{\mathcal{F}}}^2(x, y) \sum_{z=-M_z}^{M_z} (s_{\mathcal{F}}(x, y) - s(x, y, z)) \right) \quad (4)$$

$$s_{\mathcal{F}}(x, y) = \max_{-\delta_z \le z \le \delta_z} (s(x, y, z)) \quad (5)$$

where M_z is the tolerance bound $(2m)$ and δ_z the z-step $(0.25m)$. Finally, the **CP**-value is higher when the correlation profile has got a high (because of the square function) and unique peak nearby the facet (because of the sum of the relative differences).

3.2 A Structured Feature Coherence Analysis

A complementary way to assess the roof facet consistency is to take advantage of the high level of structuration of urban areas. Extracting these structures from the images allows us to verify the facet geometric characteristics and the shape description correctness. Hence, 3D segments detected from images provide positive clues when they overlap the facet edges or lay onto its plane, but also negative ones when they are found in a corner, or far away.

Edgel Extraction First, the detected contours are matched in order to produce robust, accurate and very low-level linear feature elements (Fig. 4) by using the reconstruction technique proposed in (Jung et al., 2002). These features, called "edgels", are 3D points with a 3D tangent direction. Here, the facet is only used to determine the regions of interest in the images and the matching process is performed with photogrammetrical constraints. The corresponding contours are searched in a reliable and adaptative tolerance bound estimated thanks to a DEM. This bound is larger when the features are closer to the DEM discontinuities. Thus, the main structures of the scene can be extracted even if the facet is not correct.

Figure 4: Reconstruction of edgels applied on an under-modelled facet. On the left, edgels projected on one image. On the right, a 3D view of the edgel set. The main structures of the roof building are well reconstructed wherever image contours have been extracted.

3D Segment Detection A set of relevant 3D segments are extracted from the edgel set in order to compare them to the facet. A filtering method enables to recover the segment direction and location, applied firstly in planimmetry and secondly in altimetry. Geometrical and filtering thresholds are required in order to get robust segments, the main ones being a required minimum number of edgels accumulated along the segment (linked to the image number). The 3D segments are detected inside three specific zones which are defined according to the facet (Fig. 5). A segment coherence value is defined for each zone.

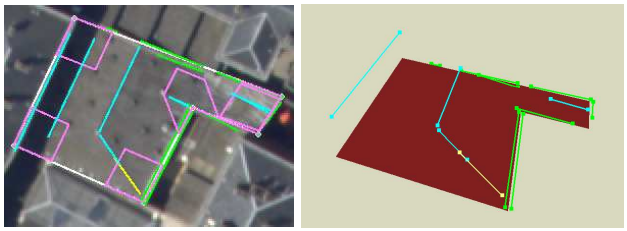

Figure 5: 3D segments detected for the under-modelled facet within three specific zones: near the edges (green), in the corners (yellow) and inside (cyan). Notice that a 3D inner segment belongs to a neighbouring facet (on its left). The corner zones are outlined in pink (on the left). In the 3D view (on the right), a 3D segment corresponding to a shadow boundary is occluded by the 3D facet. Even if many segments are detected near the facet edges, negative clues are collected by those detected in the corner and inside the facet.

Facet Edge Analysis An edge zone is defined for each facet edge with a distance and an angular deviation thresholds. The detection of 3D segments overlapping the facet edges allow to verify the facet boundary consistency and to detect over-modelling errors. An Edge Segment (**ES**) value is defined by the weigthed coverage rate of the 3D segments $\{s_{j_0}, .., s_{j_n}\}$ projected onto their corresponding facet edge e_j:

$$\mathbf{ES} = \frac{\sum_{j=0}^{n} \alpha_j r(e_j, \{s_{j_0}, .., s_{j_n}\})}{\sum_{j=0}^{n} \alpha_j \|e_j\|} \quad (6)$$

where the function r computes the coverage length, α_j is a weight parameter (1/2 for edges belonging to several facets and 1 otherwise) and $\|.\|$ is the euclidean distance between the segment end-points.

Facet Corner Analysis A corner zone is defined for each facet vertice (pink polygons in Fig. 5, left) with a window width $(5m)$

and an angular deviation threshold ($15°$). The corner segments allow to verify the facet shape correctness and to detect under-modelled roof (a missing hip roof structure for instance). A Corner Segment (**CS**) value is defined by the maximum of the summed length of the segment set $\{s_0, .., s_{j_n}\}$ detected in each corner zone j:

$$\mathbf{CS} = \max_j \sum_{i=0}^{j_n} \|s_i\| \cdot \tag{7}$$

Inner Facet Analysis The remaining edgels, that do not match with the neighbouring facet edges and that are inside the ground facet boundary, are selected in order to detect inner segments. They allow to assess the facet shape correctness. Finding a segment onto the facet plane may indicate a well localisation (the matched image contours may come from a two-material roof for instance). On the contrary, finding a segment far away from the facet plane, $2m$ above it for instance, may outline under-modelling errors, such a saw-tooth roof modelled by a flat facet. For each inner segment s_i, the area $\mathcal{A}(s_i, \mathcal{P}_\mathcal{F})$ defined between its end-points and their projection onto the facet plane is computed. This area is normalised by the length of the facet in the segment direction ($\|\mathcal{F}_{\overrightarrow{s_i}}\|$) in order to take into account the facet shape variability. Then, a Inner Segment (**IS**) value is defined by the sum of the normalised areas of all inner segments:

$$\mathbf{IS} = \sum_{i=0}^{n} \frac{\mathcal{A}(s_i, \mathcal{P}_\mathcal{F})}{\|\mathcal{F}_{\overrightarrow{s_i}}\|}. \tag{8}$$

4. FACET QUALITY SELF-DIAGNOSIS

We introduce in this section how image coherence characterization is used to classify the roof facet quality. First, four levels of quality are defined. Afterwards, a learning and a supervised classification are performed in order to associate and predict facet quality classes from the image coherence parameters.

4.1 Definition of quality classes

Four quality classes have been defined in order to value their level of adequacy with reality from false to correct:

- *false*: the roof facet does not fit with the reality (Fig. 6(a));
- *generalised*: a part of the roof is not correctly modelled or geometric deviations are observed (Fig. 6(c));
- *acceptable*: the roof is quite well modelled, but either unmodelled hip roof ridge without geometric deviation or small geometric deviations are observed (Fig. 6(d));
- *correct*: the roof is correctly modelled by the facet (Fig. 6(b)).

The self-diagnosis process should alert the *false* and *generalised* facets and validate the *acceptable* and *correct* facets.

4.2 A Supervised Classification

The problem of self-diagnosing the quality of roof facets is expressed as a classification problem, whose inputs are the quality classes and a parameter vector $\mathbf{V} = \{\mathbf{CD}, \mathbf{CP}, \mathbf{ES}, \mathbf{CS}, \mathbf{IS}\}$. A simple classifier, the k-Nearest Neighbour (Duda et al., 2000), has been used to evaluate the efficiency of the image coherence measures. Each parameter is normalised by its standard deviation computed on the training instances. The euclidean distance between two normalised parameter vectors has been used.

Practically, 60 instances of each quality class have been learnt. Fig. 7 shows parameter mean and standard deviation for each quality class. Firstly, it shows that image coherence mean values are compliant with the quality classes, as expected. Secondly, even if the class *false* is quite well disjoined from the other ones, the classes *generalised* and *acceptable* are really close from each other. Indeed, these two labels are assigned whether a facet is acceptable or not, based on its shape correctness and geometrical accuracy. Finally, it shows that no measure alone is able to reliably classify each quality class.

(a) class *false* (b) class *correct*

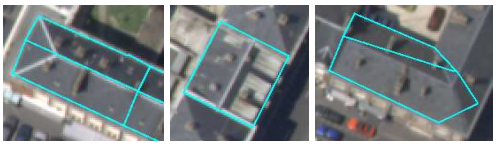

(c) class *generalised*

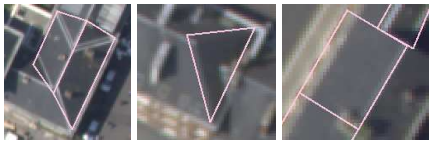

(d) class *acceptable*

Figure 6: Some facet instances of each quality class. The *false* and *generalised* ones should be identified as not acceptable by the self-diagnosis algorithm.

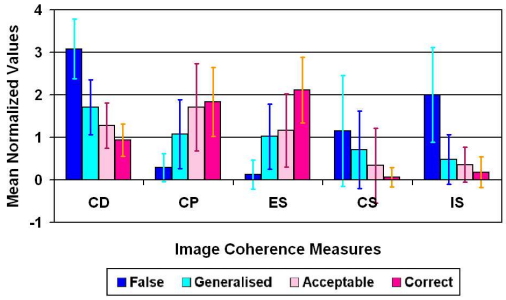

Figure 7: Image coherence parameter mean and standard deviation for each quality class when applied on the training instances.

4.3 Robust Decision Rules

In the following, the neighbour number k has been fixed to 15 which is a good trade-off between overfitting and generalisation. As the majority vote rule is not robust enough and does not reveal ambiguous classifications, the final decision is taken in order to translate the self-diagnosis results into the three classes of the traffic light paradigm. The decision is based on the number of neighbours N_F, N_G, N_A, N_C belonging to each class, the distance d of the k neighbours, and follows selective rules for acceptance:

- if ($N_F + N_G \geq \frac{k}{2}$ or $\max(N_F, N_G) \geq \frac{k}{3}$) :
  if the majority vote says F or G, decide *Rejected*;
  otherwise, decide *Undecided*,
- if ($N_F + N_G \geq \frac{k}{3}$ or $d \geq \beta k$) : decide *Undecided*,
- otherwise: decide *Accepted*.

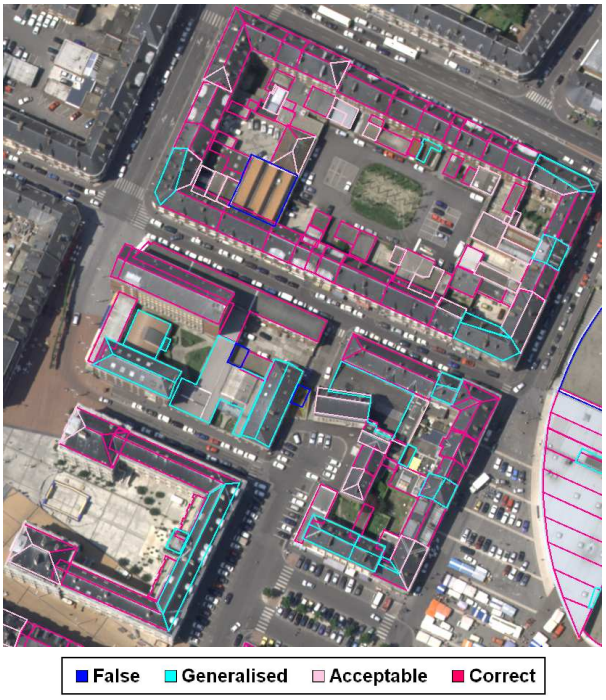

Figure 8: Manually labelled roof facets of the realistic dataset.

Figure 9: Correct (detected/validated) and incorrect (not detected/to be checked) self-diagnosis decisions of the realistic dataset.

Here, the maximum distance of all the neighbours has been fixed with $\beta = 1.2$. Moreover, neighbours at a distance null have been excluded, enabling to merge the results of the training and testing examples in the next section.

5. RESULTS

5.1 3D Building Model Datasets

We have chosen two dense urban areas of Amiens, France. The first one is composed of many similar buildings, mainly with gable roofs, hip roofs and low slope garage roofs within courtyards. The second area is composed of many different roof materials and shapes, with a mix of industrial and very small buildings.

Two building model datasets have been used for the self-diagnosis evaluation. The first one, called realistic (Fig. 8), has been produced semi-automatically by a platform containing several algorithms (Flamanc and Maillet, 2005). The main modelling errors (nearly 20% on 862 facets) are hip roof with missed structures, industrial buildings simply modelled by a flat roof and small buildings poorly modelled. In order to get enough modelling errors for statistical evaluation, we complete the first dataset with a second one simulating systematic errors and containing only flat roof facets (80% incorrect facets on 251). They have been delimited by 2D vectorial building footprints and are located at the median altitude given by a DEM. As buildings have many different shapes, the simulated discrepancies between the reality and the models are widespread. All roof facets that are flat in the realistic dataset have been removed from the flat roof dataset. This one provides all the training instances of the class *false* and a few ones of the class *generalised*, while the realistic dataset provides all the other ones.

5.2 Quantitative Results

As regards to the semi-automatic building model verification, an operator will inspect the *rejected* and *undecided* facets. Thus, the self-diagnosis process makes two erroneous decisions : a False Acceptance (FA) error when a *false* or *generalised* facet is classified as *accepted*, and a False Rejectance (FR) error when an *acceptable* or *correct* facet is classified as *rejected* or *undecided*. It should be emphasis that minimizing the FA errors is the most important because the *accepted* facets will not be inspected anymore. FR errors only correspond to time lost for an operator to inspect facets while ideally it would not have been required.

The results of the self-diagnosis algorithm are provided in Table 1 merging all the facets of both datasets. The percentages are computed according to the facet number of each quality class. The self-diagnosis algorithm detects almost all the *false* modelling errors (0.5% FA rate), but the results are mixed with the class *generalised* (nearly 20% FA rate) which is confused with the classes *acceptable* (11%) and *correct* (9%). As the decision rule is selective for acceptance, only 52% and 80% of correct acceptance rates are reached for the classes *acceptable* and *correct* respectively. Globally, the rates of correct rejectance (91%) and correct acceptance (73.7%) are quite satisfying, especially considering that an overall rate of 79.6% of correct decisions is reached with only 3% of false acceptance errors on the whole datasets (containing 1113 roof facets).

Quality class	Decision			Facet number
	Rejected	*Undecided*	*Accepted*	
	Correct R.		FA error	
false	96.2%	3.3%	0.5%	209
generalised	63.5%	17.1%	19.4%	170
	FR error		Correct A.	
acceptable	28.9%	19.1%	52%	173
correct	9.4%	10.2%	80.4%	561

Table 1: The statistics of the self-diagnosis decisions according to the quality class on the whole datasets.

5.3 Qualitative Results

An overview of the correct and incorrect self-diagnosis decisions is provided on the realistic dataset (Fig. 9). It shows that many facets are correctly classified. As regards to the false rejectance decisions (Fig. 10), the facet quality estimation is generally mislead either by occlusions, by the presence of shadows, dormer-windows or a hip roof ridge without geometric deviation. Even if these facets have been manually labelled as *acceptable* or *correct*, their inspection by an operator may be well-founded - for some of them at least-.

Figure 10: Examples of false rejectance decisions from the realistic dataset.

Let's now focus on the analysis of the false acceptance decisions. Considering the results presented in Fig. 9, only 4 false acceptance decisions have been made on 33 incorrect facets. In figure 11(a), the facet is geometrically accurate but a hip roof structure is not modelled. This is not detected by corner segments because the unmodelled roof ridge is not contrasted enough. Therefore, no evidence of incorrectness shape description has been proved (as for 13 FA errors on 34). In figure 11(b), a part of an overhanging roof is modelled by the facet of interest. The roof slope and location are correct, its boundary is covered at 44% by edge segments. As the corner segment directions do not fit with the roof ridge, no corner segment has been detected. Therefore, using the pseudo-median function and based on the detected segments, this facet has been erroneously validated. In figure 11(c), a double side roof is modelled by an horizontal facet. Even if the middle ridge is detected by inner segments (IS = 2.6), fair geometric deviation measurement (CD = $50cm$) and edge segment coverage (ES = 50%) lead to its validation. In figure 11(d), the roof slope is deviated by the neighbouring roof. While the CD value is quite the same, smaller CP value and edge coverage (ES = 28%) are balanced by a very small inner segment value (IS = 0.2). Finally, based on 10 neighbours belonging to the class *acceptable*, this facet has been validated.

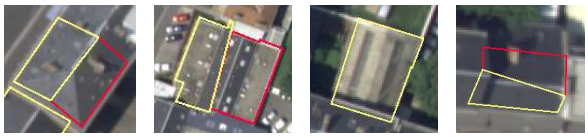

(a) a missing hip roof structure

(b) an extended roof

(c) an under-modelled roof

(d) a deviated slope roof

Figure 11: Examples of false acceptance decisions (yellow outlined) from the realistic dataset.

6. CONCLUSION AND PERSPECTIVES

We have introduced a new approach for a quality self-diagnosis of roof facets in dense urban areas. It is based on the definition of robust and meaningful image-driven measures that aims at characterizing individual roof facet existence and consistency. The originality of our work is to take advantage of a set of very low-level image observations and of a supervised learning in order to classify roof facet quality. Although a simple classifier is used, it has shown very promising results in the difficult context of dense urban areas with the detection of almost all the *false* modelling errors (99.5%). Considering also the *generalised* modelling errors, which should be alerted, the evaluation shows very satisfyingly that only 3% of false acceptance decision is made on the whole datasets. Our efforts will be focused on the improvement of the *generalised* facet detection (only 81%) while keeping a good correct acceptance rate.

Future works will be carried out on the completion of the image coherence measures by considering the radiometric changes between the images and the change consistency with the facet specular direction. It will allow us to assess the slope of the roof facets when the roof material is not lambertian. Besides, others classifiers could be used, as linear separation or neural networks for instance, in order to improve the classification stage.

7. ACKNOWLEDGEMENTS

The author would like to acknowledge the French Defence Agency (DGA) for supporting this research.

REFERENCES

Ameri, B., 2000. Feature based model verification (FBMV): A new concept for hypothesis validation in building reconstruction. In: Proceedings of the XIXth ISPRS Congress, IAPRS, Vol. 33, B3, Amsterdam.

Duda, R., Hart, P. and Stork, D., 2000. Pattern Classification. Wiley Interscience.

Durupt, M. and Taillandier, F., 2006. Automatic building reconstruction from a digital elevation model and cadastral data : An operational approach. In: Proceedings of the ISPRS Commission 3 Symposium on Photogrammetric Computer Vision, Bonn, Germany.

Flamanc, D. and Maillet, G., 2005. Evaluation of 3D city model production from pleiades-HR satellite images and 2D ground plans. In: 3rd International Symposium Remote Sensing and Data Fusion over Urban Areas, Tempe, USA.

Förstner, W., 1994. Diagnotics and performance evaluation in computer vision. In: Performance versus Methodology in Computer Vision, NSF/ARPA Workshop, IEEE Computer Society, Seattle.

Förstner, W., 1996. 10 pros and cons against performance characterization of vision algorithms. In: Workshop on Performance Characteristics of Vision Algorithms, Cambridge.

Henricsson, O. and Baltsavias, E., 1997. 3-D building reconstruction with ARUBA: a qualitative and quantitative evaluation. In: Automatic Extraction of Man-Made Objects from Aerial and Space Images (II), Ascona, pp. 65–76.

Jibrini, H., Pierrot-Deseilligny, M., Paparoditis, N. and Matre., H., 2004. Détermination d'une surface polyédrique continue optimale à partir d'un fouillis de plans. In: RFIA' 04, Vol. 1, AFRIF-AFIA, Toulouse, France.

Jung, F., Tollu, V. and Paparoditis, N., 2002. Extracting 3d edgel hypotheses from multiple calibrated images: a step towards the reconstruction of curved and straight object boundary lines. In: Proceedings of the ISPRS Photogrammetric Computer Vision, IAPRS, Vol. 34, Graz, Austria, pp. B100–104.

Kim, Z. and Nevatia, R., 2003. Expandable bayesian networks for 3d object description from multiple views and multiple mode inputs. IEEE Transactions on Pattern Analysis and Machine Intelligence 25(6), pp. 769–774.

Kim, Z. and Nevatia, R., 2004. Automatic description of complex buildings from multiple images. Computer Vision and Image Understanding 96(1), pp. 60–95.

McKeown, D., Bulwinkle, T., Cochran, S., Harvey, W., McGlone, C. and Shufelt, J., 2000. Performance evaluation for automatic feature extraction. In: Proceedings of the XIXth ISPRS Congress, IAPRS, Vol. 33, Amsterdam, pp. 379–394.

Meidow, J. and Schuster, H., 2005. Voxel-based quality evaluation of photogrammetic building acquisitions. In: CMRT'05, Vienna.

Paparoditis, N., Thom, C. and Jibrini, H., 2000. Surface reconstruction in urban areas from multiple views of aerial digital frames. In: Proceedings of the XIXth ISPRS Congress, IAPRS, Vol. 33, B3, Amsterdam.

Rottensteiner, F. and Schulze, M., 2003. Performance evaluation of a system for semi-automatic building extraction using adaptable primitives. In: IAPRS, Vol. 34, Munich.

Schuster, H.-F. and Weidner, U., 2003. A new approach towards quantitative quality evaluation of 3d building models. In: J. Schiewe, L. Hahn, M. Madden and M. Sester (eds), ISPRS com IV, Workshop "Challenges in Geospatial Analysis, Integration and Visualization II", Stuttgart, Germany, pp. 156–163.

Suveg, I. and Vosselman, M., 2002. Mutual information based evaluation of 3D building models. In: 16th International Conference on Pattern Recognition (ICPR 02), Vol. 3, IAPR/IEEE Computer Society, Quebec city, pp. 557–560.

Taillandier, F. and Deriche, R., 2004. Automatic buildings reconstruction from aerial images: a generic bayesian framework. In: Proceedings of the XXth ISPRS Congress, IAPRS, Istanbul.

Thacker, N., Clark, A., Barron, J., Beveridge, R., Clark, C., Courtney, P., Crum, W. and Rameh, V., 2005. Performance characterization in computer vision : A guide to best practices.